

From ground state energies towards excitation for extended quantum systems

Markus Holzmann

LPMMC, CNRS UGA Grenoble

- Ground state energies (electron gas, He^4):
iterated backflow, neural network wave functions
- Energy gaps (insulators):
single particle excitations (charged gap)
particle-hole excitations (neutral gap)
- Fermi liquid properties (metals):
momentum distribution
renormalization factor Z
effective mass m^*

Trial wave functions: Many-body correlations (U_n with $n > 2$)

Variational principle for ground state energies:

$$E_0(N) \leq E_T(N) \equiv \frac{\langle \Psi_T | H | \Psi_T \rangle}{\langle \Psi_T | \Psi_T \rangle}$$

Analytical forms/ efficient calculations:

- Most general 3body form

$$U_3(\mathbf{R}) = \sum_{i < j < k} u_3(\mathbf{r}_{ij}, \mathbf{r}_{ik})$$

- Local energy method suggests

$$U_3[\mathbf{R}] = \sum_i \sum_{j,k} \mathbf{r}_{ij} \cdot \mathbf{r}_{ik} u_3(r_{ij}) u_3(r_{ik}) = \sum_i \left[\sum_j \mathbf{r}_{ij} u_3(r_{ij}) \right] \cdot \left[\sum_k \mathbf{r}_{ik} u_3(r_{ik}) \right]$$

- Introduce generalized vector/tensor forms

“backflow vector” $\mathbf{d}_i = \sum_{j \neq i} \mathbf{r}_{ij} d(r_{ij})$ 1D functions to be optimized

“backflow tensor” $\underline{T}_i |_{\alpha\beta} = \sum_{j \neq i} \mathbf{r}_{ij} |_{\alpha} \mathbf{r}_{ij} |_{\beta} t(r_{ij})$ $\alpha = x, y, z$

- **n-body correlations** must be scalars:

$$U_3 = \lambda \sum_i \mathbf{d}_i \cdot \mathbf{d}_i \quad U_4 = \sum_i \mathbf{d}_i \cdot \underline{T}_i \cdot \mathbf{d}_i$$

n-body backflow $\mathbf{x}_i = \underline{T}_i \mathbf{d}_i$

- easily automatized
- Chain rules for derivatives
- 1D function per vector/tensor
- Computational cost remains $\sim N^2$

Backflow network from path integral method

Ruggeri, Moroni, M.H., Phys. Rev. Lett. 120, 205302 (2018).

$$\Psi_\tau(\mathbf{R}) \sim \int d\mathbf{R}' \exp [-\lambda(\mathbf{R} - \mathbf{R}')^2 - V(\mathbf{R}) - U(\mathbf{R}')]$$

Perform integration of hidden layers approximately

by expanding U around some (arbitrary) point Q $U(\mathbf{R}') \approx U(\mathbf{Q}) + (\mathbf{R}' - \mathbf{Q})\nabla U(\mathbf{Q})$

$$\Psi_\tau(\mathbf{R}) \approx \int d\mathbf{R}' \exp [-\lambda(\mathbf{R}' - \mathbf{R} + \nabla U/2\lambda)^2 - V(\mathbf{R})] \times \exp [-U(\mathbf{Q}) - (\mathbf{R} - \mathbf{Q}) \cdot \nabla U + (\nabla U)^2/4\lambda]$$

choose Q at the center of the gaussian (small $\tau \equiv$ large λ)

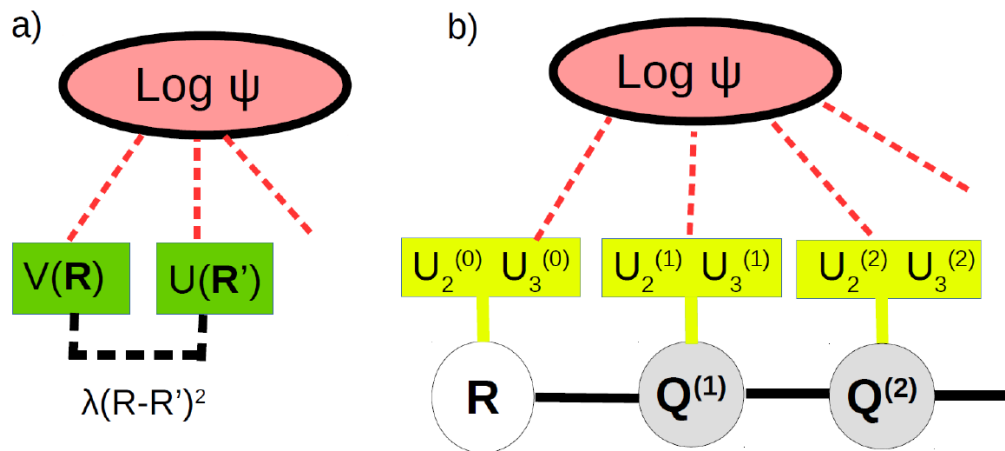
=> implicit determination of Q by

$$\mathbf{Q} = \mathbf{R} - \nabla U(\mathbf{Q})/2\lambda \rightarrow \mathbf{q}_i \simeq \mathbf{r}_i - \sum_{j \neq i} \mathbf{r}_{ij} \eta(r_{ij})$$

$$\Psi_\tau(\mathbf{R}) \sim \exp [-V(\mathbf{R}) - U(\mathbf{Q}) - (\nabla U)^2/4\lambda]$$

and iterate.....

⇒ Backflow network

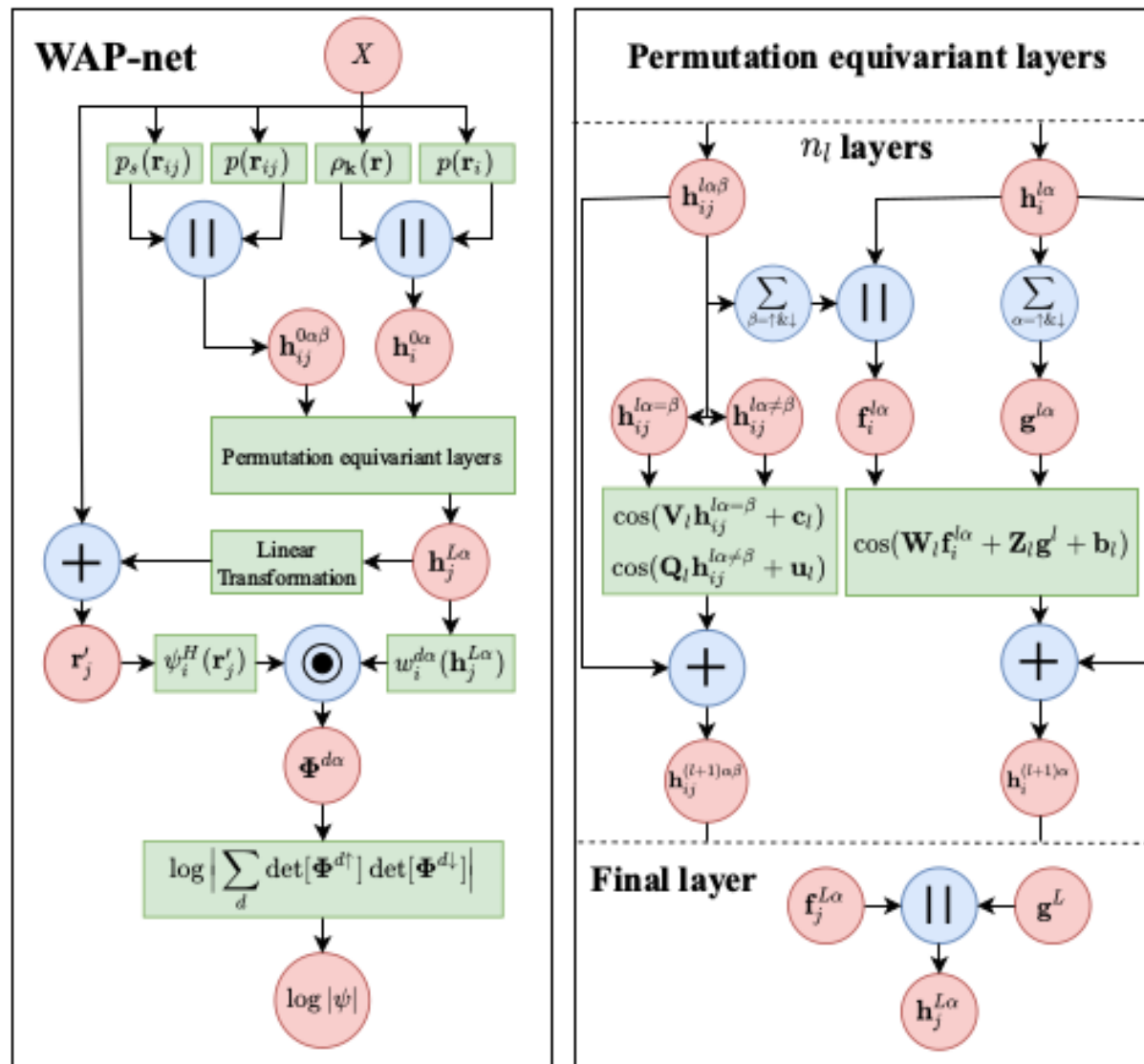


exponential convergence for “smooth” potentials...

fermionic determinants are not smooth....

Neural network based wave functions: WAP-net

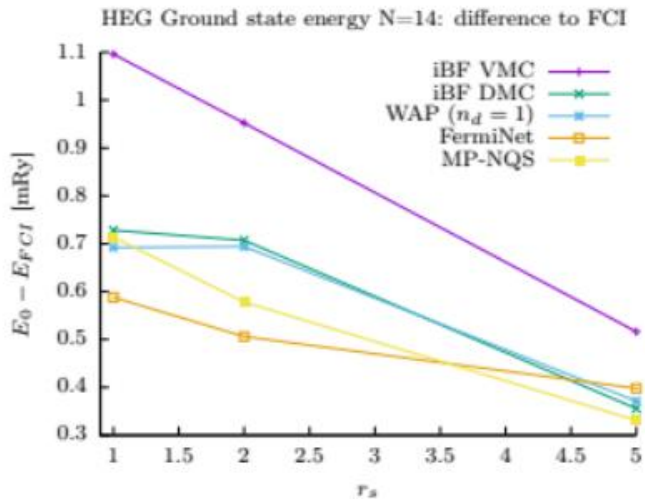
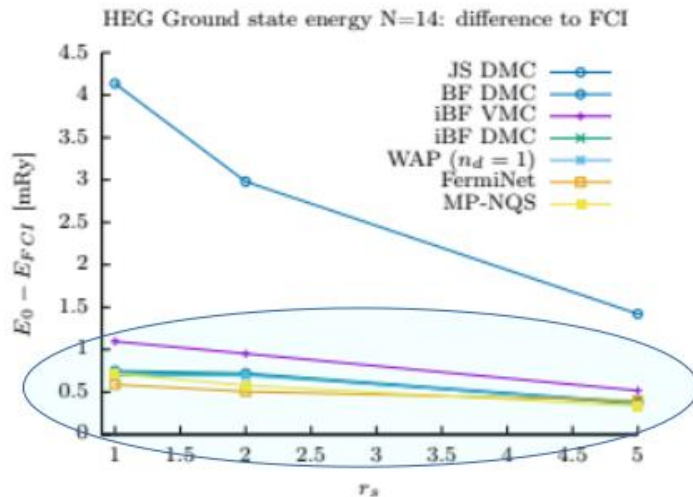
M. Wilson, S. Moroni, M. H., N. Gao, F. Wudarski, T. Vegge, A. Bhowmik
Phys. Rev. B 107, 235139 (2023).



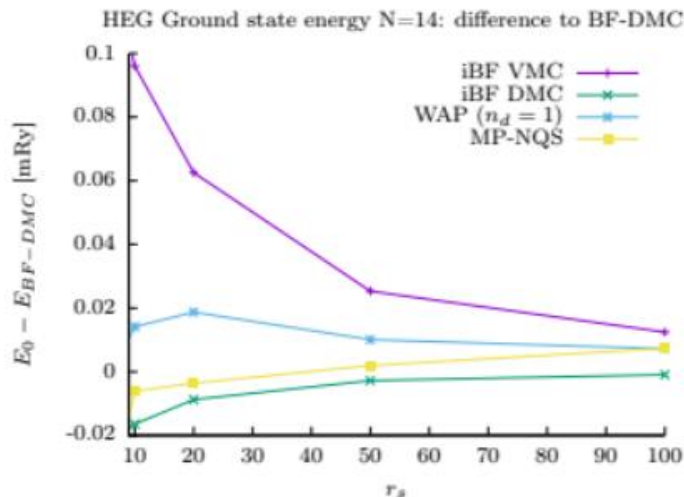
Benchmark HEG N=14

IBF, WAP-net, FermiNet, MP-NQS, FCI...

High density $r_s < 5$



low density $r_s > 5$



FCI:

K. Liao, T. Schraivogel, H. Luo, D. Kats, A. Alavi, Phys. Rev. Research 3, 033072 (2021).

FermiNet:

G. Cassella, H. Sutterud, S. Azadi, N. D. Drummond, D. Pfau, J. S. Spencer, W. M. C. Foulkes, Phys. Rev. Lett. 130, 036401 (2023).

MP-NQS:

G. Pescia, J. Nys, J. Kim, A. Lovato, G. Carleo, arXiv 2305.07240 (2023).

Application of iterated backflow renormalization: Polarization (Stoner) transition in the HEG?

M.H. and S. Moroni, Phys. Rev. Lett. 124, 206404 (2020)

Many-body correlations in the low Density region can be accurately Extrapolated by iterative backflow

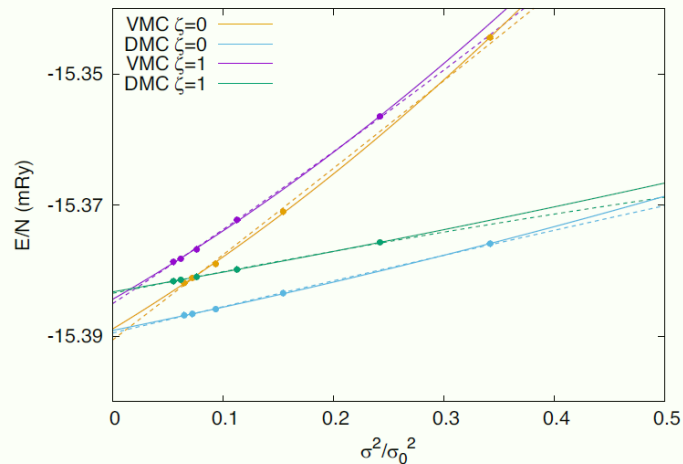


FIG. 1. Extrapolation of the energy to zero variance for $r_s = 100$ at polarizations $\zeta = 0$ and 1. The data are calculated with VMC and DMC using SJ, BF0, ..., BF4 wave functions in order of decreasing energy. The reference value σ_0^2 is the variance of the local energy at $\zeta = 0$ with the SJ wave function. The curves are quadratic fits; for each set of data points (VMC and DMC for $\zeta = 0$ and 1) there are two curves, one of which (solid line) excludes the SJ energy from the fit.

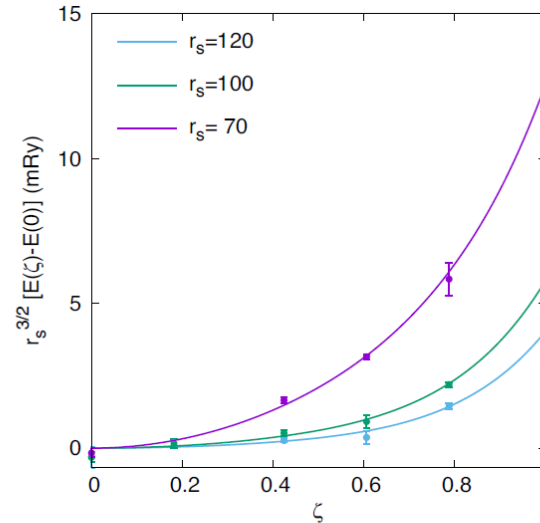
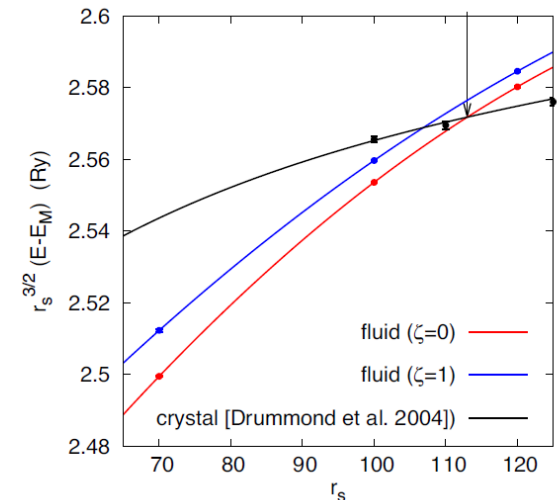


FIG. 3. The polarization energy $E(\zeta) - E(0)$ obtained from zero-variance extrapolations of the DMC energies without the SJ result. The lines are polynomial fits with terms of order 0, 2, and 6. Alternative functional forms and ensuing confidence levels for

Wigner crystalzation sets in before Polarization transition



Does a Stoner transition occur in nature?

- **Electronic systems:**
itinerant ferromagnetism: **correlations** + **band structure**
- different **isotropic** systems with **spin-independent** ?
(ultracold atoms/ molecules)
 - Change scattering length $a_s \rightarrow \infty$?
=> difficulties/controversals due to 2-body bound state leading to instability!
 - Dipolar interactions (heteronuclear molecules, Rydberg atoms)?
=> no polarization transition in 2D before freezing

T. Comparin, R. Bombin, M. H., F. Mazzanti, J. Boronat, and S. Giorgini,
Phys. Rev. A 99, 043609 (2019)

Conjecture:

For an isotropic normal Fermi liquid with
spin-independent isotropic interactions
the ground state remains unpolarized up to freezing.

Liquid/solid He⁴ at T=0

- Hamiltonian for He⁴ atoms interacting via Aziz pair potential

$$H = \sum_i \frac{p_i^2}{2m} + \sum_{i<j} v(r_{ij})$$

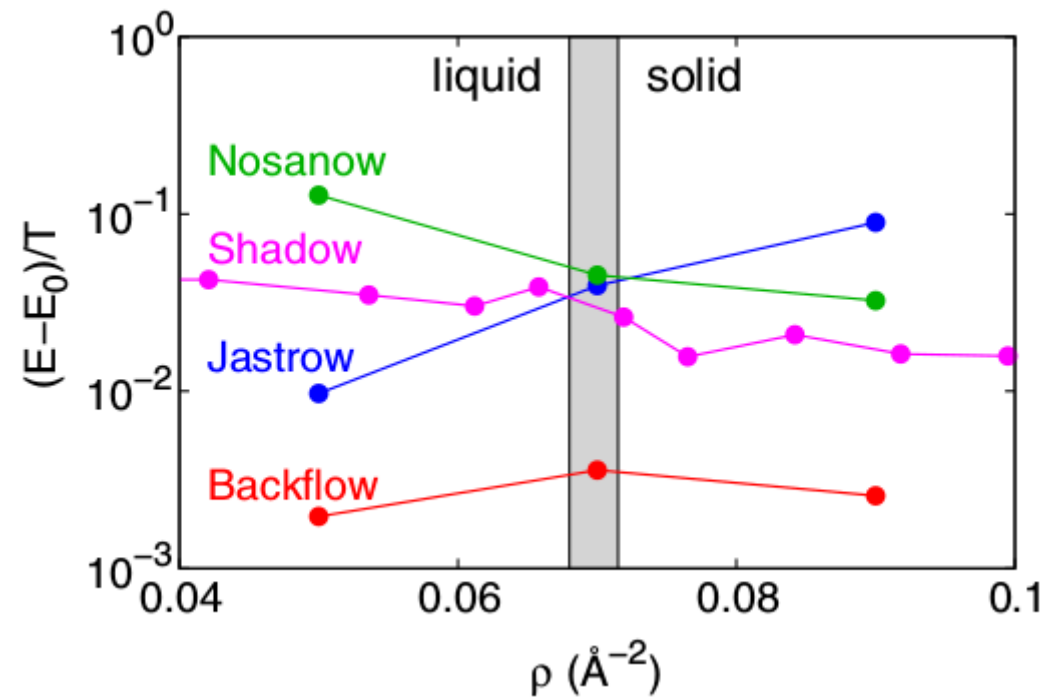
- Iterated backflow describes liquid-solid transition with translational invariant wavefunctions

Ruggeri, Moroni, M.H., Phys. Rev. Lett. 120, 205302 (2018).

- Benchmark of **MPNN (graph) network** in 2D

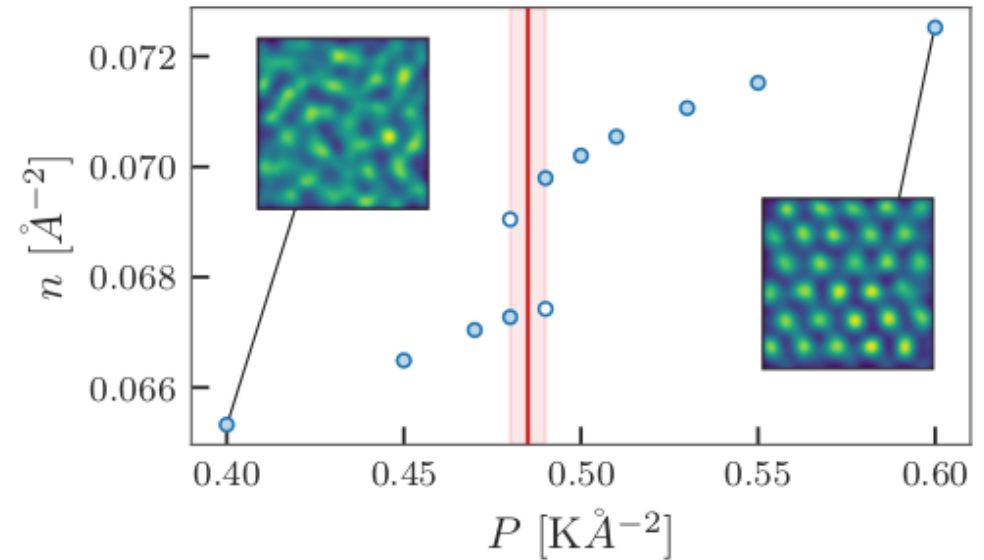
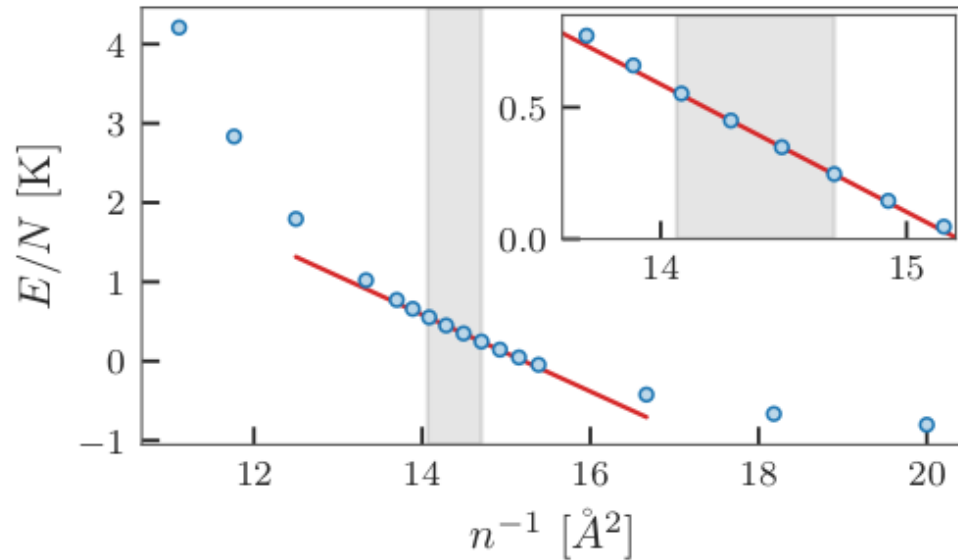
↙

N	n [Å ⁻²]	E_{VMC}/N [K]	σ^2/N [K ²]	E_{DMC}/N [K]
16	0.05	-0.8357(5)	0.06	-0.8347(4)
	0.075	0.8672(4)		0.879(2)
	0.09	3.952(2)	0.66	3.955(1)
30	0.05	-0.8026(8)	0.08	-0.8022(5)
	0.065	-0.0336(6)		-0.042(1)
	0.075	1.048(1)		1.021(2)
	0.09	4.209(3)	0.60	4.208(3)
48	0.05	-0.7963(8)	0.05	-0.7960(5)
	0.065	-0.0241(3)		-0.023(1)
	0.075	1.0677(8)		1.05(1)
	0.09	4.2725(4)		4.29(1)



Liquid/solid He⁴ at T=0: Going into the (forbidden) mixture region

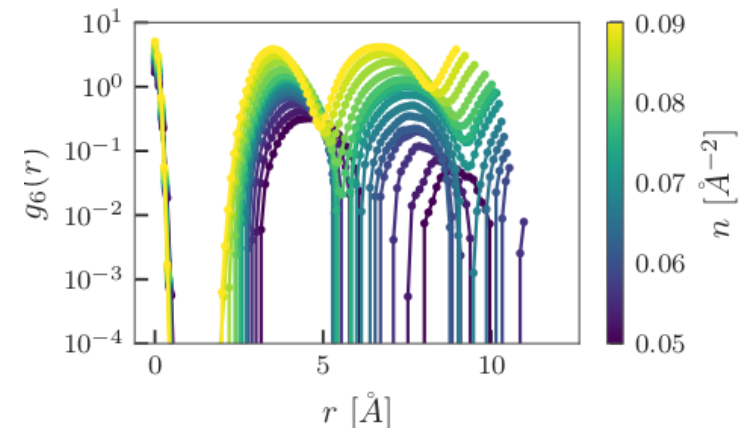
D. Linteau, G. Pescia, J. Nys, G. Carleo, M. H. (in preparation)



An old question: Is there a phase with hexatic order?

$$g_6(r) = \langle \Psi_6^*(\mathbf{r}_i) \Psi_6(\mathbf{r}_j) \rangle, \quad \Psi_6(\mathbf{r}_i) = \frac{1}{6} \sum_{j \in \mathcal{N}_6(i)} e^{6i\theta_{ij}}$$

- $g_6(r \rightarrow \infty) \sim \text{cst.}$ → solid,
- $g_6(r) \sim r^{-\eta}$ → hexatic,
- $g_6(r) \sim e^{-r/\xi}$ → liquid,



N likely too small to be conclusive....

From ground states to excitations.....

Excitation spectra of insulators (I): single-particle (charge) excitation gap

Y. Yang, V. Gorelov, C. Pierleoni, D. Ceperley, M. H., Phys. Rev. B 101, 085115 (2020)

- consider perfect crystal with fixed number N_p of ions
add and subtract electrons $N = \dots, N_p - 1, N_p, N_p + 1, \dots$ (+ background charge)

$$\Delta = E_0(N_P + 1) + E_0(N_P - 1) - 2E_0(N_P) \quad (\text{fundamental gap})$$

contains only ground state energies (variational)

- Impose twisted boundary conditions on wave functions $\Psi(\mathbf{r}_1 + L_x \hat{x}) = e^{i\theta_x} \Psi(\mathbf{r}_1)$.

$$f = \frac{1}{M_\theta V} \sum_{\theta} \min_N [E_0(N, \theta) - \mu N] \quad (\text{"grand-canonical" } N \text{ vs } \mu)$$

- Can be extended to include nuclear quantum/thermal motion (phonons)

V. Gorelov, D. M. Ceperley, M. H., C. Pierleoni, J. Chem. Phys. 153, 234117 (2020);

- Coulomb size effects

$$\Delta V = \frac{1}{2} \left[\int \frac{d^3 \mathbf{k}}{(2\pi)^3} - \frac{1}{V} \sum_{\mathbf{k} \neq 0} \right] \frac{4\pi e^2}{k^2} [S(k) - 1]$$

$$S_k^\pm \equiv (N_e \pm 1)S_{N_e \pm 1}(k) - N_e S_{N_e}(k) \quad \lim_{k \rightarrow 0} S_k^\pm = \alpha_\pm + \mathcal{O}(k^2),$$

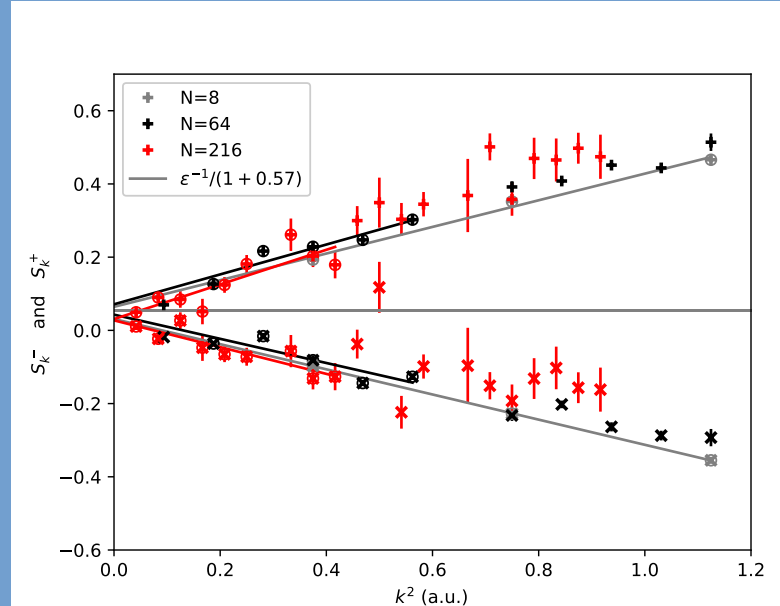
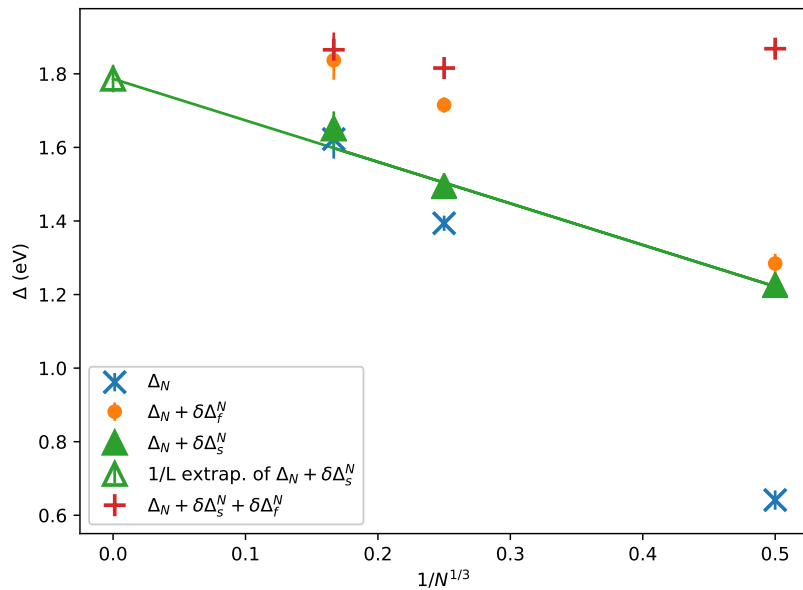
- Size effects for gap:

$$\left[\int \frac{d^3 k}{(2\pi)^3} - \frac{1}{V} \sum_{\mathbf{k} \neq 0} \right] \frac{v_k}{2} S_k^\pm \simeq \alpha_\pm \frac{|v_M|}{2} \sim L^{-1} \sim N_e^{-1/3}$$

- General

$$\Delta_\infty - \Delta_V = \frac{|v_M|}{\epsilon} + \mathcal{O}\left(\frac{1}{V}\right)$$

Si diamond (test case)



Excitation spectra of insulators (II): particle-hole (neutral) excitation gap

Gorelov, Yang, Ruggeri, Ceperley, Pierleoni, M.H. Condens. Matter Phys. 26, 33701 (2023); cond-mat/2303.17944.

Size effects depend on localized/extended character

- **Localized** e-h excitation (exciton): $\Delta_\infty - \Delta_N \sim \frac{1}{N}$
- **extended** e-h excitation (inter-band transitions): $\Delta_\infty - \Delta_N \sim \frac{1}{L} \sim \frac{1}{N^{1/3}}$

Localization of e-h pairs
needs supercells larger to localization length

$$L \gtrsim 2l_x$$
$$l_X \sim \frac{\hbar^2 \epsilon}{m_X e^2}$$

Excitonic size effects can be estimated based on
dielectric constant and effective band mass

$$\Delta_n(\infty) - \Delta_n(L) = \frac{|v_M(L)|}{\epsilon} - \frac{|v_M(2l_X)|}{\epsilon}$$

Hydrogen: Phase I (hcp): electronic gap from QMC vs experiment

V. Gorelov, M.H., D. M. Ceperley, C. Pierleoni, Phys. Rev. B 109, L241111

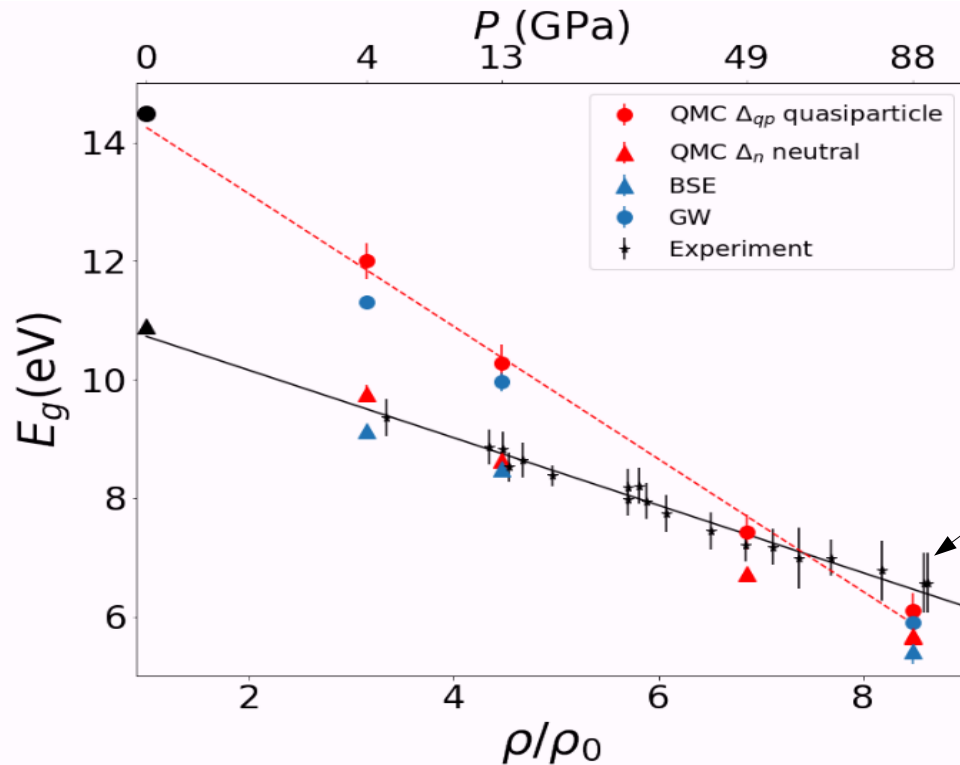


FIG. 1. Comparison between room temperature experimental data and theoretical predictions for the electronic gap of solid hydrogen in phase I as a function of compression. Experimental data are from ref. [16]. We report quasi-particle and neutral gap from QMC (red symbols, quasiparticle circles, neutral triangles) and from MBPT (blue symbols, circles BSE, triangle GW) both corrected for finite size effects. Reference density value ρ_0 corresponds to $r_{s_0} = 3.2413$. The continuous line is the fit to experimental data: $E_g(\rho/\rho_0) = 11.3 - 0.57(\rho/\rho_0)$.

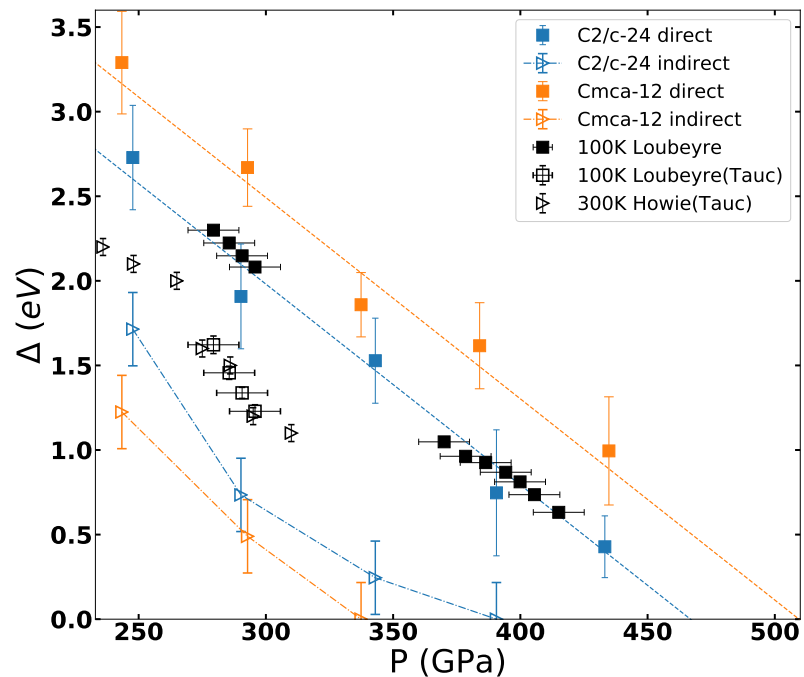
Experimental results from
inelastic X-ray scattering:

Gap from lower limit of photon
energy loss spectra

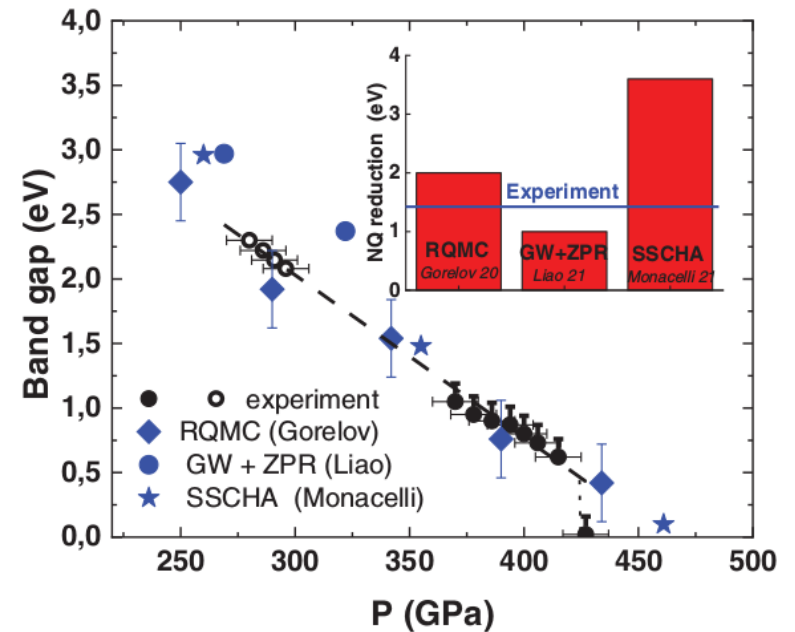
B. Li, Y. Ding, D. Y. Kim, L. Wang, T.-C. Weng, W. Yang, Z. Yu, C. Ji, J. Wang, J. Shu, J. Chen, K. Yang, Y. Xiao, P. Chow, G. Shen, W. L. Mao, H.-K. Mao, *Probing the Electronic Band Gap of Solid Hydrogen by Inelastic X-Ray Scattering up to 90 GPa*, Physical Review Letters 126, 36402 (2021).

High pressure hydrogen: Insulator-metal transition

- Characterize insulator:
spectral (optical) properties, gaps,...



V. Gorelov, M. Holzmann, D. Ceperley,
C. Pierleoni, PRL 124, 116401 (2020)



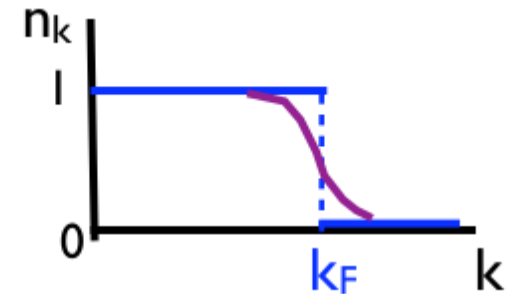
P. Loubeyre, F. Occelli, P. Dumas,
PRL 129, 035501 (2022)

Landau-Fermi Liquid (I)

Ideal Fermions:

occupation number:
Fermi-Dirac distribution

$$n_{k\sigma} = \frac{1}{e^{(\hbar^2 k^2 / 2m - \mu) / T} + 1}$$



- Observation:

Low $T_{\text{temperature}}$ Properties of a Fermi **liquid** (^3He)
 \approx **ideal** Fermi gas with **renormalized** parameters

- Interacting Fermions postulating **quasi-particles**:

single particle dispersion with effective mass m^* $\varepsilon_{k\sigma}^0 = \frac{\hbar^2 k_F}{m^*} (|\mathbf{k}| - k_F)$

$$E(\delta n_{k\sigma}) = E_0 + \sum_{k,\sigma} \varepsilon_{k\sigma}^0 \delta n_{k\sigma} + \frac{1}{2V} \sum_{k\sigma k'\sigma'} f_{k\sigma, k'\sigma'} \delta n_{k\sigma} \delta n_{k'\sigma'} + \dots$$

quasi-particle interactions, **necessary** for consistency!

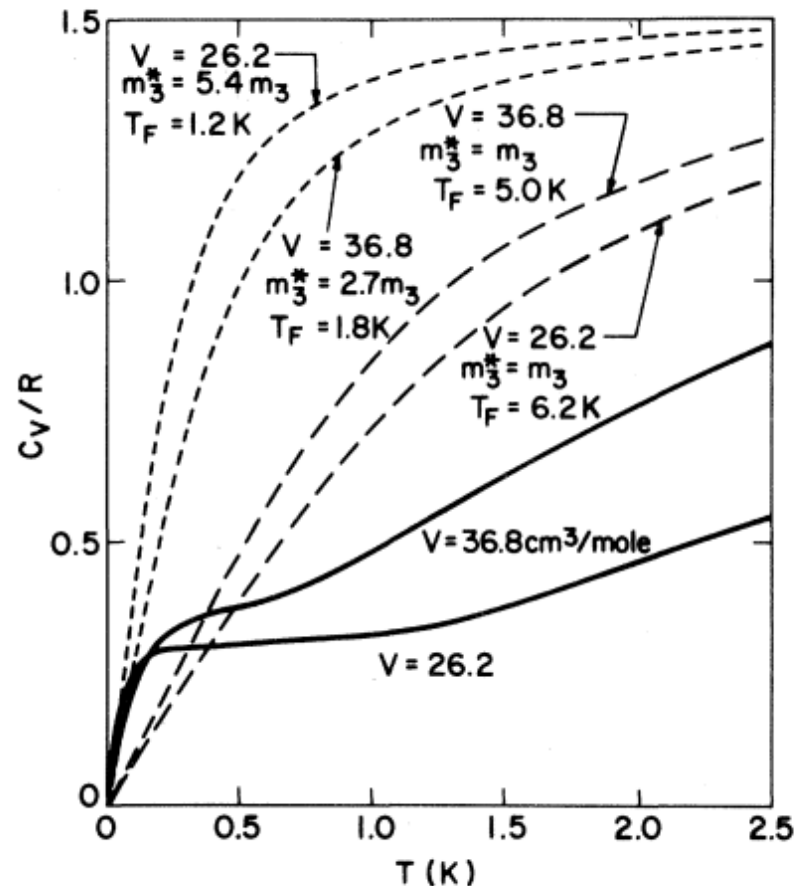
Landau-Fermi Liquid (II)

- quasi-particle occupation $\delta n_{\mathbf{k}}$:
 - adiabatically connected to ideal gas occupation
 - not directly observable
- parameters [m^* , $f(\mathbf{k}, \mathbf{k})$] at k_F determined by few measurements (specific heat C , compressibility, magnetic susceptibility,...)
 - ⇒ predictions for transport properties, ...

➔ Limits of applicability?

specific heat of liquid ^3He

D. Greywall PRB 27, 2747 (1983)



Fermi Liquid: Microscopic Description (I)

Single particle Green's function: $G_R(k, t) \equiv -i \langle e^{iHt} a_k e^{-iHt} a_k^\dagger \rangle \theta(t)$

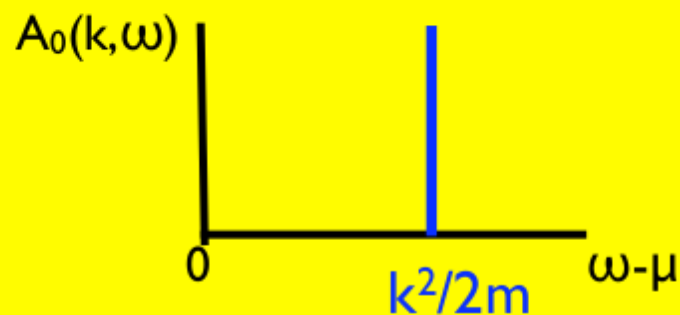
$$G_R(k, \omega) = \sum_n \frac{|\langle n | a_k^\dagger | 0 \rangle|^2}{\omega - (E_n^{N+1} - E_0^N - \mu) + i\eta} = \int \frac{d\omega}{2\pi} G_R(k, \omega) e^{-i\omega t}$$

excitation energies \implies peaks in spectral function

$$A(k, \omega) = -\frac{1}{\pi} \text{Im} G_R(k, \omega) \quad (\text{measured in ARPES})$$

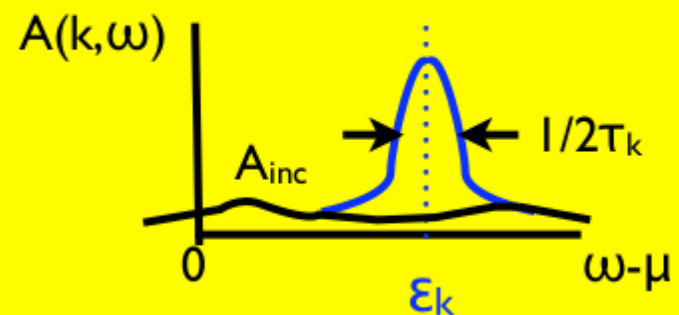
ideal gas

$$A_0(k, \omega) = \delta(\omega - \mu - k^2/2m)$$



interacting system

$$A_0(k, \omega) = \frac{Z_k}{2\pi} \frac{\tau_k^{-1}}{(\omega - \mu - \epsilon_k)^2 + (2\tau_k)^{-2}} + A_{\text{inc}}$$



Fermi Liquid: Microscopic Description (II)

Self-energy $\Sigma(k, \omega)$: $G^{-1}(k, \omega) = \omega - \mu - k^2/2m - \Sigma(k, \omega)$

form of G around
quasi-particle peak

$$G^{-1}(k, \omega - \mu \approx \varepsilon_k) = Z_k^{-1}(\omega - \mu - \varepsilon_k + i\tau_k/2)$$

quasi-particle energy: $\varepsilon_k = k^2/2m + \text{Re} \Sigma(k, \mu + \varepsilon_k)$

inverse quasi-particle weight: $Z_k^{-1} = 1 - \partial \text{Re} \Sigma(k, \mu + \varepsilon_k) / \partial \omega$

inverse lifetime: $\tau_k^{-1} = -2Z_k \text{Im} \Sigma(k, \mu + \varepsilon_k)$

Definition of Fermi liquid: $\tau_k^{-1} \rightarrow 0$ for $k \rightarrow k_F$

Delta function excitation
at the Fermi surface $A(k \rightarrow k_F, \omega \approx \mu) = Z_k \delta(\omega - \mu - k^2/2m^*)$

$$m/m^* = Z_{k_F} (1 + m/k_F \partial \Sigma(k_F, \mu) / \partial k)$$

with effective mass m^* from expansion around $\omega - \mu = \varepsilon_k \equiv k^2/2m^*$

$$\Sigma(k, \mu + \varepsilon_k) = \Sigma(k_F, \mu) + (k - k_F) \partial \Sigma(k_F, \mu) / \partial k + \varepsilon_k \partial \Sigma(k_F, \mu) / \partial \omega + \dots$$

Fermi Liquid: Momentum Distribution n_k

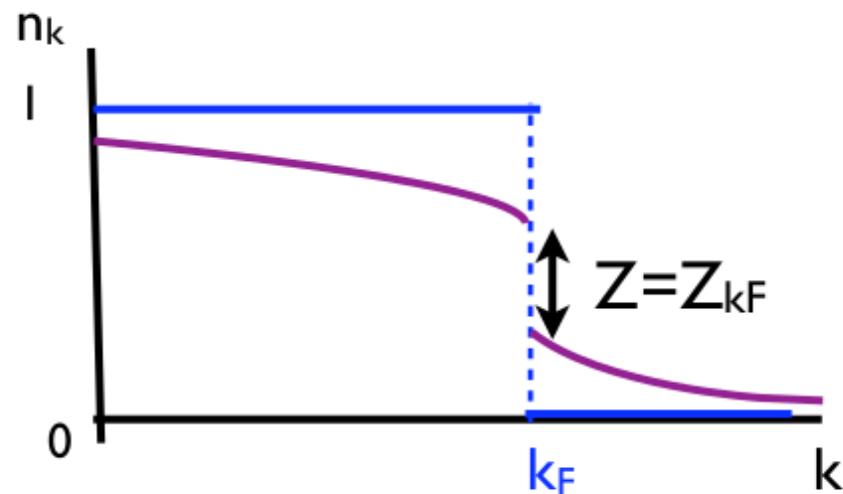
Sharp jump of n_k at k_F is consequence of δ -function excitation at k_F

$$n_k \equiv \langle a_k^\dagger a_k \rangle = \int_{-\infty}^{\mu} d\omega A(k, \omega)$$

$k < k_F$: quasi-particle peak of A **below** μ

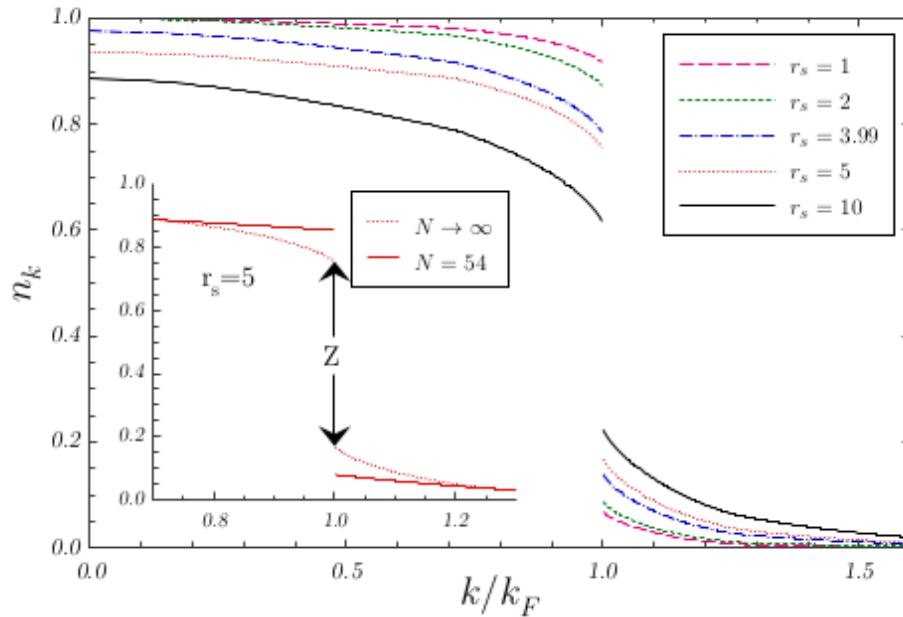
$k > k_F$: quasi-particle peak of A **above** μ

$$n_k - n_p \simeq Z_k + \int_{-\infty}^{\mu} d\omega [A_{inc}(k, \omega) - A_{inc}(p, \omega)]$$



n(k), Z of jellium (3DEG) at various densities

M.H., B. Bernu, C. Pierleoni, J. McMinis, D.M. Ceperley, V. Olevano, L. Delle Site, PRL **107**, 110402 (2011) (2011).

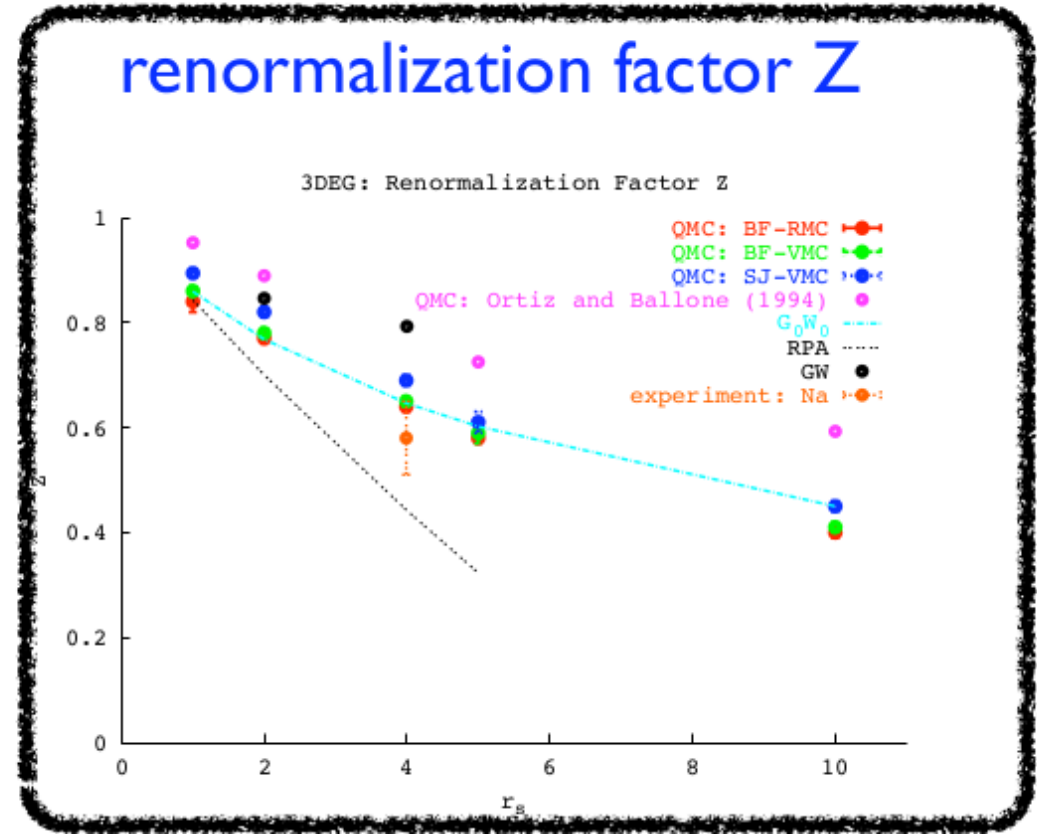


from analytical expressions of Ψ :
exact behavior of n_k around k_F

Quantitative agreement of QMC with G_0W_0
 over broad density region ($1 \leq r_s \leq 5 \dots 10$)

r_s	1	2	3.99	5	10
BF-RMC	0.84(2)	0.77(1)	0.64(1)	0.58(1)	0.40(1)
SJ-VMC	0.894(9)	0.82(1)	0.69(1)	0.61(2)	0.45(1)
BF-VMC	0.86(1)	0.78(1)	0.65(1)	0.59(1)	0.41(1)
G_0W_0 [25]	0.859	0.768	0.646*	0.602	0.45
GW_0 [26]		0.804	0.702*		
GW [27]		0.846	0.793*		
Lam [28]	0.896	0.814	0.615*	0.472	
RPA [28]	0.843	0.700	0.442*	0.323	
SJ-DMC [6]	0.952	0.889		0.725	0.593

renormalization factor Z



[25] L. Hedin, Phys.Rev. **139**, A796 (1965).

[26] U. von Barth, B. Holm, PRB **54**, 8411 (1996).

[27] B. Holm, U. von Barth, PRB **57**, 2108 (1998).

[28] J. Lam, PRB **3**, 3243 (1971).

[6] G. Ortiz, P. Ballone, PRB **50**, 1391 (1994).

Renormalization factor Z

Best QMC: BF-RMC

M. H., B. Bernu, C. Pierleoni, J. McMinis, D. M. Ceperley, V. Olevano, and L. Delle Site, Phys. Rev. Lett. 107, 110402 (2011).

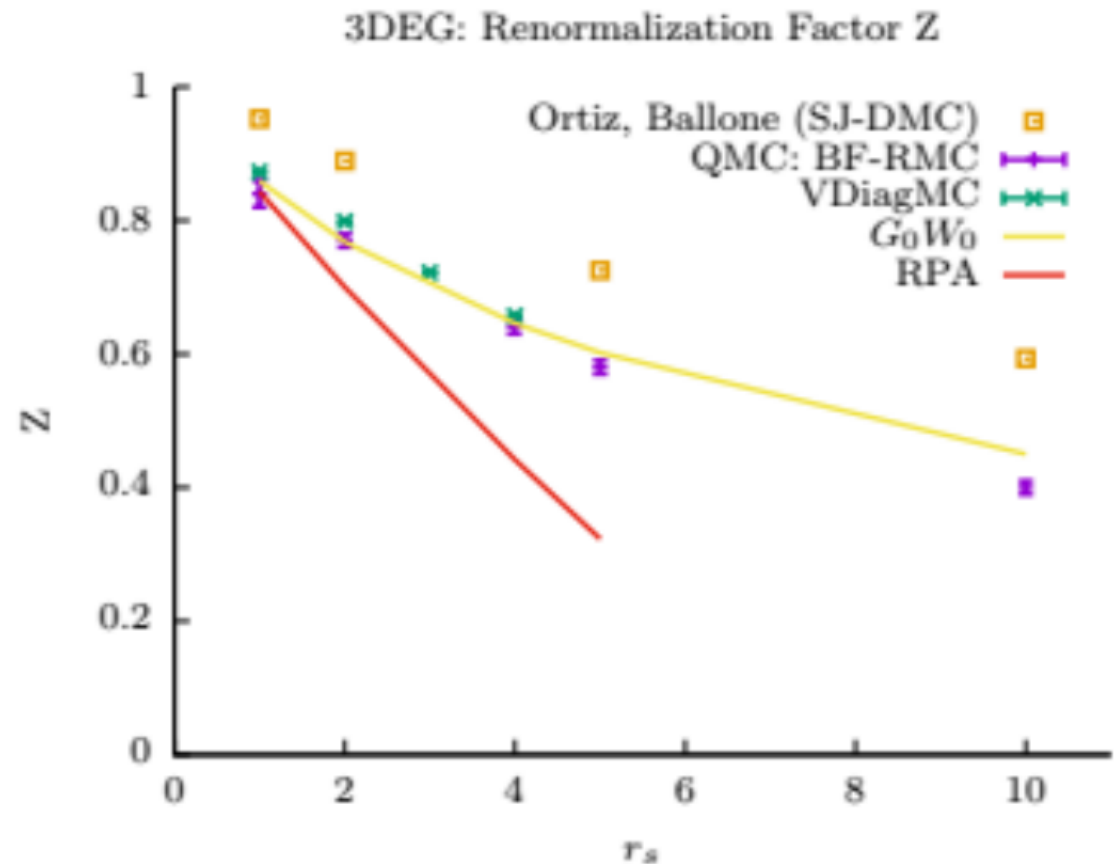
- Comparisons:

- RPA

- G_0W_0

- beyond G_0W_0 : Variational diagramatic Monte Carlo (VDiagMC)

K. Haule and K. Chen, Scientific Reports 12, 2294 (2022).



Effective mass m^*

- **Controversy:**
VdiagMC, K. Haule and K. Chen,
Scientific Reports 12, 2294 (2022)
vs QMC study by
Azadi, Drummond, Foulkes
PRL 127, 086401 (2021)
- **However:**
QMC based on assumptions
for Landau energy functional
VdiagMC based on Green's function

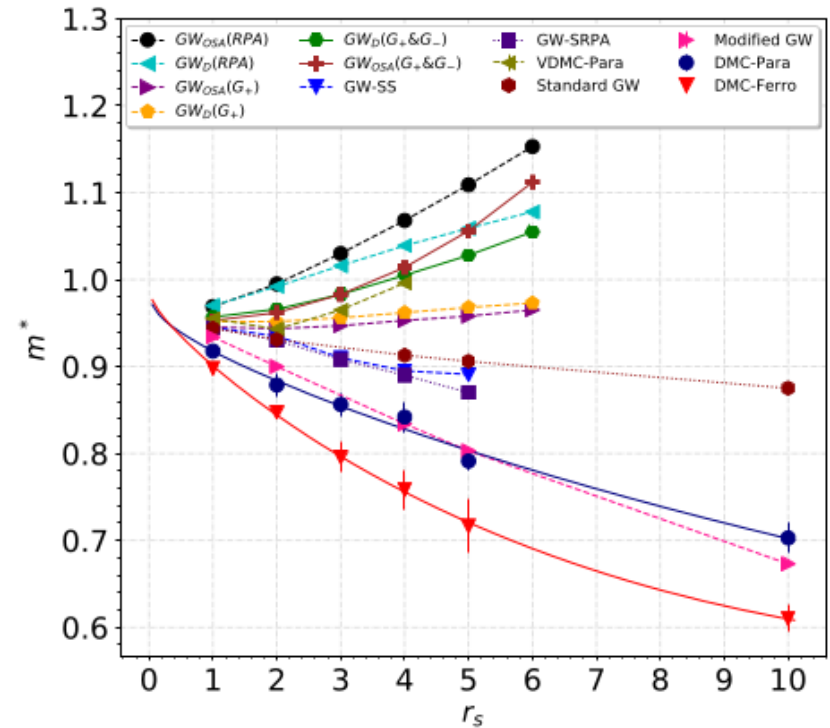


FIG. 4. Quasiparticle effective masses m^* of paramagnetic (Para) and ferromagnetic (Ferro) 3D HEGs at the infinite-system-size limit as functions of density parameter r_s . Padé functions were fitted to the DMC quasiparticle energy bands to determine the effective mass. The many-body GW_x and variational diagrammatic Monte Carlo (VDMC) results are from Refs. [52] and [53], respectively. The GW SS and GW SRPA results are from Refs. [54] and [55], respectively. The “standard GW ” data and “modified GW ” data are taken from Ref. [56]. All the GW results are for paramagnetic 3D HEGs.

$$\delta E = \sum_{p\sigma} (\varepsilon_p + \mu) \delta n_{p\sigma} + \frac{1}{2V} \sum_{p\sigma, p'\sigma'} f(p\sigma, p'\sigma') \delta n_{p\sigma} \delta n_{p'\sigma'}$$

major problem with mapping of QMC trial-wave function to **phenomenological** Landau functional

$$E(\delta m_k) = E_0 + \sum_k \varepsilon_k^0 \delta m_k + \frac{1}{2V} \sum_{k\sigma k'\sigma'} f_{k\sigma, k'\sigma'} \delta m_k \delta m_{k'} + \dots$$

definition of δm_k only unique for lowest energy state with different total momentum

2 extrapolations:

- $N \rightarrow \infty$
- $k \rightarrow k_F$

\equiv 2 major difficulties !

for any system size, N ,
only very few states
close to the Fermi surface
can be used

(basically states with infinite lifetime!)

(does $N \rightarrow \infty$, $k \rightarrow k_F$ commute?)

\rightarrow need for new QMC methodology for m^*

Microscopic Definition of m^*

Def. from single particle
Green's function $\frac{m}{m^*} = \frac{1 + \frac{m}{k_F} \frac{\partial \Sigma(k_F, \mu)}{\partial k}}{1 - \frac{\partial \Sigma(k_F, \mu)}{\partial \omega}}$

Fermi liquids have jump Z in
momentum distribution: $Z = \frac{1}{1 - \frac{\partial \Sigma(k_F, \mu)}{\partial \omega}}$

✗ we calculate Z within QMC

□ how to calculate k-derivative of self-energy? $\frac{\partial \Sigma(k_F, \mu)}{\partial k}$

↳ note that $\Sigma(k, \mu)$ is a **static** quantity

and $G(k, \mu)$ is a **static response** function!

QMC calculation of the static self-energy (I)

QMC can calculate static response function remaining variational

VOLUME 69, NUMBER 13

PHYSICAL REVIEW LETTERS

28 SEPTEMBER 1992

Static Response from Quantum Monte Carlo Calculations

Saverio Moroni,^{(1),(a)} David M. Ceperley,⁽¹⁾ and Gaetano Senatore⁽²⁾

⁽¹⁾*National Center for Supercomputing Applications and Department of Physics,
University of Illinois at Urbana-Champaign, Urbana, Illinois 61801*

⁽²⁾*Dipartimento di Fisica Teorica, Università di Trieste, Strada Costiera 11, I-34014 Trieste, Italy*

(Received 18 June 1992)

$$v_{\text{ext}}(\mathbf{r}) = 2v_{\mathbf{q}} \cos(\mathbf{q} \cdot \mathbf{r}),$$

$$E_v = E_0 + \frac{\chi(q)}{n_0} v_{\mathbf{q}}^2 + C_4 v_{\mathbf{q}}^4 + \dots$$

adapt for single particle excitation:

add external potential ξa_k^\dagger to Hamiltonian $H(\xi_k) = H - \mu N + \xi_k a_k^\dagger + \xi_k^* a_k$

and minimize energy using N/N+1 wave function $E(\xi_k) - E_0 = G(k, \mu) \xi_k^2$

\Rightarrow static self-energy $\Sigma(k, \mu) = \mu - G^{-1}(k, \mu) - k^2/2m$

QMC calculation of the static self-energy (II)

$$H(\xi_k) = H - \mu N + \xi_k a_k^\dagger + \xi_k^* a_k$$

$$E_0(\xi_k) \leq \frac{\langle \Psi_k | H(\xi_k) | \Psi_k \rangle}{\langle \Psi_k | \Psi_k \rangle}$$

ansatz for wave function: $\Psi_k(\mathbf{R}) = \psi_0^N(\mathbf{R}_N) + \alpha_k \psi_k^{N+1}(\mathbf{R}_{N+1})$

$$E_0(\xi_k) = E_0 - \frac{z_k}{E_k^{N+1} - E_0^N - \mu} \xi_k^2, \quad \text{for } \xi_k \rightarrow 0$$

$$z_k = \frac{|\langle \psi^{N+1} | a_k^\dagger | \psi_0^N \rangle|^2}{\langle \psi_0^N | \psi_0^N \rangle \langle \psi_k^{N+1} | \psi_k^{N+1} \rangle} \quad E_k^{N+1} = \frac{\langle \psi_k^{N+1} | H \psi_k^{N+1} \rangle}{\langle \psi_k^{N+1} | \psi_k^{N+1} \rangle}$$

chose wave function such that:

- a) minimize energy difference $E_k^{N+1} - E_0^N - \mu$ $\phi_k^{N+1}(\mathbf{R}_{N+1}) = \det_{ik} \varphi_k(\mathbf{q}_i) e^{-U_{N+1}}$
- b) maximize overlap z_k $a_k^\dagger \psi_0^N(\mathbf{R}_N)$

Static self-energy

M.H., F. Calcavecchia, D.M. Ceperley, V. Olevano, PRL 131, 186501 (2023) (2023)

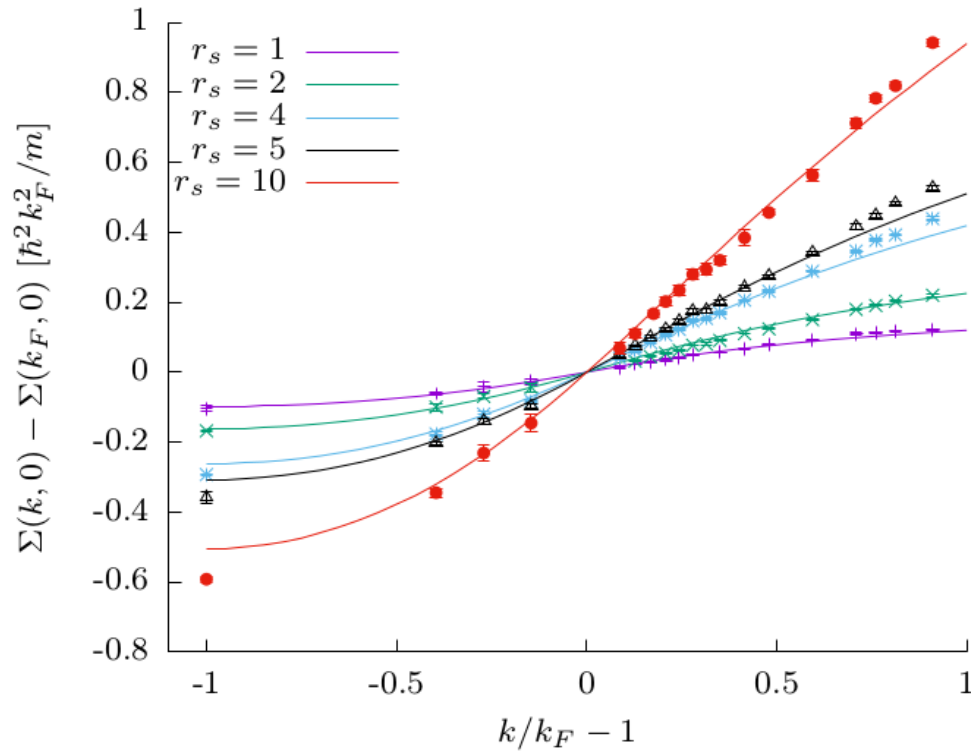


FIG. 1: Static self-energy for various densities (r_s) using backflow (BF) trial wave functions and GC-TABC simulations for $N = 38$ electrons. They include size corrections. The color lines are from G_0W_0 calculations.

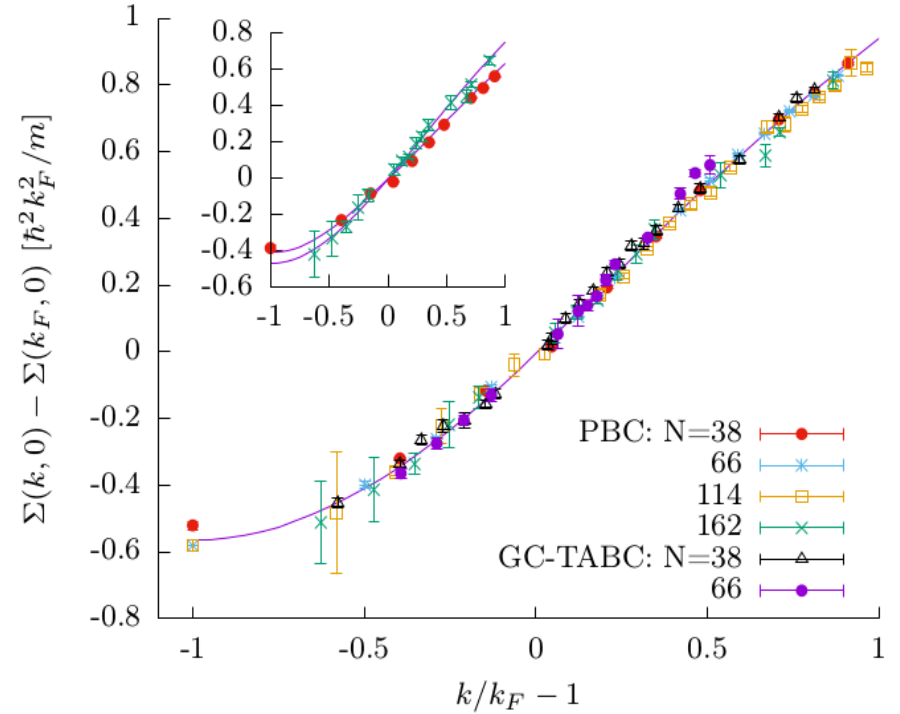


FIG. 2: Static self-energy for $r_s = 10$ using SJ-VMC trial wave functions for simulations with periodic boundary conditions (PBC) and GC-TABC for various sizes ranging from $N = 38$ to $N = 162$, size corrected according to Eq. (17), the line is a fit to the data. The inset shows the uncorrected values for $N = 38$ and $N = 162$ (PBC), the lines indicate the size corrections of the fit based on Eq. (17).

Size corrections (analytic):

M. H., B. Bernu, D. Ceperley, J. Phys.: Conf. Ser. 321 012020 (2011), cond-mat/1105.2964.

4.2. Renormalization factor and effective mass

For the calculation of the renormalization factor and the effective mass, we need the derivatives of the self energy at the Fermi surface. Within the RPA, we have

$$\frac{\partial \Sigma(k_F, \varepsilon_F)}{\partial \omega} = -\frac{1}{V} \sum_{\mathbf{q} \neq 0} \int_{-\infty}^{\infty} \frac{d\nu}{(2\pi)} \left[\frac{1}{\epsilon(q, i\nu)} - \frac{1}{\epsilon(q, 0)} \right] \frac{v_q}{[i\nu + \varepsilon_F - \varepsilon_{k_F+\mathbf{q}}]^2} \quad (19)$$

$$\frac{m}{k_F} \frac{\partial \Sigma(k_F, \varepsilon_F)}{\partial k} = \frac{1}{V} \sum_{\mathbf{q} \neq 0} \int_{-\infty}^{\infty} \frac{d\nu}{(2\pi)} \frac{1}{\epsilon(q, i\nu)} \frac{v_q}{[i\nu + \varepsilon_F - \varepsilon_{k_F+\mathbf{q}}]^2} \left[1 + \frac{\mathbf{k}_F \cdot \mathbf{q}}{k_F^2} \right] \quad (20)$$

➔ Leading order size corrections from Coulomb singularity ($q \rightarrow 0$)

Exact (beyond RPA) leading order finite size corrections (based on Ward identities):

$$\delta \Sigma(k, 0) \simeq - \int_{-\pi/L}^{\pi/L} \frac{d^3 q}{(2\pi)^3} \int_{-\infty}^{\infty} \frac{d\nu}{(2\pi)} \frac{v_q}{\epsilon(q, i\nu)} \frac{1}{i\nu + \mu - \varepsilon_{k+q}^0}$$

Summary - Conclusions:

- ⇒ Improvement of ground state wave functions: iterated backflow, machine learned network ansätze...
- ⇒ He⁴ solid-liquid, solid-hexatic-liquid?
- ⇒ Gaps: single particle and p-h excitations, size effects, S(k)....
- ⇒ Fermi Liquid parameters: Z, m*

David Linteau
(EPFL Lausanne)

Yubo (Paul) Yang
Flatiron, NY

Saverio Moroni
(CNR, SISSA, Trieste)

Vitaly Gorelov
(CNR, Palaiseau)

David Ceperley
(UIUC)

Valerio Olevano
(Néel, Grenoble)

Carlo Pierleoni
(University of L'Aquila)

Max Wilson
(DTU)

Giuseppe Carleo
(EPFL Lausanne)